PHYSICAL REVIEW D VOLUME 9, NUMBER 3 1 FEBRUARY 1974

Consequences of the scale-invariant parton model for deep-inelastic neutrino scattering

A. Casher,* J. Kogut, and Leonard Susskind
Tel Aviv University, Ramat Aviv, Tel Aviv, Israel
(Received 20 June 1973)

The scale-invariant parton model is used to obtain the consequences of short-distance scale invariance for deep-inelastic neutrino processes. We first generalize the model to incorporate quantum numbers. The moments of structure functions are power-behaved functions of Q^2, thus violating Bjorken scaling in a systematic way. We find that the total neutrino cross section and the average neutrino energy loss scale canonically. However, the mean squared momentum $\langle Q^2 \rangle$ divided by the neutrino energy E falls as a power of E, thus providing a sensitive test of the breakdown of canonical scaling. Furthermore, the ratio of neutrino to antineutrino cross sections on particular hadrons is predicted to approach unity at extreme energies. These results are compared with those of other theories of the breakdown of canonical scaling.

I. INTRODUCTION

In the near future deep-inelastic weak and electromagnetic experiments will test the validity of various theories of the short-distance behavior of strong interactions. Until now the experimental success of the Bjorken scaling hypothesis has been the dominant theoretical idea in constructing such theories. However, it is becoming clear from theoretical studies that canonical scaling may not be consistent with renormalizable local field theories.[1] The reason for this is that in renormalizable theories more and more structure is uncovered at shorter and shorter distances.[2] We will, therefore, suppose that at some higher energies and momentum transfers these new features will manifest themselves. One hypothesis which is particularly attractive and tractable is that the short-distance behavior of strong interactions is scale-invariant. Bjorken scaling is an example of scale invariance in which the short-distance behavior becomes characteristic of massless free-field theory. Another possibility for scale-invariant short-distance behavior is that the interactions become characterized by dimensionless cutoff-independent parameters. The second possibility and not the first is supported by studies of renormalizable field-theory models.[3] The conventional parton model which leads to Bjorken scaling is based on free-field short-distance behavior. Recently we have formulated a modified parton approach to scale-invariant field theories which are not free at short distances.[4]

In this paper we discuss the implications of the scale-invariant parton model to neutrino-nucleon interactions, assuming that the weak interactions are adequately described by the conventional current-current interaction. Of course, at truly extreme energies the structure of the weak interaction itself will change. Our approach only becomes relevant if there is a region in energy in which deviations from canonical scaling are significant but corrections to the current-current interaction are not yet important. The calculations made here should indicate the directions of the breakdown of canonical scaling before energies are reached where the simple Fermi form of weak interactions fails.

We will first discuss two theoretical issues. We generalize the scale-invariant parton model to incorporate discrete quantum numbers. We find noncanonical scaling properties for the moments of structure functions as in Ref. 4. Then we analyze the role and validity of the impulse approximation in lepton-hadron scattering. We then turn to experimental questions and apply the model to deep-inelastic neutrino reactions. Assuming the conventional Fermi form of weak interactions, we find that the total neutrino-nucleon cross section rises linearly with the neutrino energy E as in the Bjorken-scaling case.[5] The average lepton energy loss in neutrino-nucleon collisions, $\langle \nu(E) \rangle$, also rises linearly with E.[6] Since these results are identical to those of the conventional parton model, the quantities $\sigma^{\nu}(E)$ and $\langle \nu(E) \rangle$ cannot distinguish between canonical and the more general scale-invariant dynamics discussed here. The unconventional results we obtain include the following: (1) The ratio of neutrino to antineutrino cross sections off particular hadrons, $\sigma^{\nu}(E)/\sigma^{\bar{\nu}}(E)$, should approach unity at extreme energies. (2) The average invariant lepton momentum transfer squared divided by the neutrino energy, $\langle Q^2/2E \rangle$, falls with energy as E^p, $-1 < p < 0$. We close with a discussion of these results and some remarks on the validity of SU(3) at short distances. In contrast with Bjorken scaling, which applies when ν and Q^2 exceed typical hadronic masses, the results of the scale-invariant parton model are expected to apply only when $\ln Q^2$ becomes large. At best we expect

that under National Accelerator Laboratory conditions only the initial deviations from canonical scaling in the directions discussed here will be observable.

II. THE SCALE-INVARIANT PARTON MODEL AND DISCRETE QUANTUM NUMBERS

We begin by reviewing some relevant features of the scale-invariant parton model. The idea of this approach is that physics at every length scale has a relevant approximate pointlike-parton description in the infinite-momentum frame. As the wavelength of an external probe decreases, we begin to uncover structure within the partons. This structure can be described with a new parton model whose elements are an order of magnitude smaller than the original partons. Hence we are led to introduce a sequence of scales (R_N) which gives the sizes of smaller partons inside bigger partons, etc. In other words, as the resolving power of external weak and electromagnetic probes increases, partons of size R_N are resolved into partons of smaller size, R_{N+1}. For this reason we will refer to the partons as clusters. As in Ref. 4, we choose the length scale R_N to be of order Λ^{-N}, where Λ is a large number. When an external probe of transverse momentum Q interacts with the hadron, transverse distances of order Q^{-1} are resolved. Hence, clusters of size $R_N \sim Q^{-1}$ absorb the external momentum. This leads to a connection between N and Q:

$$N = \frac{\ln(Q/\xi)}{\ln\Lambda} , \tag{1}$$

where ξ is a fixed, small momentum scale.

We shall be interested in the longitudinal-momentum distribution functions of clusters of type N within a hadron. Label each cluster by a discrete index i which denotes the quantum numbers it carries, such as helicity, charge, isospin, etc. Define the function $F_i(\eta, N)/\eta$ to be the average number of clusters of type N and quantum numbers i which carry longitudinal fraction η of the hadron. The distribution function $F_i(\beta, N+1)/\beta$ can be computed from $F_j(\eta, N)/\eta$ and a function $f^{ij}_{N+1,N}(\beta/\eta)/(\beta/\eta)$ which is the probability per unit β/η to find a cluster of type $(N+1, i)$ and longitudinal fraction β in a cluster of type N and longitudinal fraction η:

$$\frac{F_i(\beta, N+1)}{\beta} = \int_0^1 \frac{f^{ij}_{N+1,N}(\beta/\eta)}{(\beta/\eta)} \frac{F_j(\eta, N)}{\eta} \frac{d\eta}{\eta} . \tag{2}$$

As discussed in Ref. 4, the assumption of scale invariance means that $f^{ij}_{N+1,N}(\beta/\eta)$ becomes independent of N for large N. Denote the function as $f^{ij}(\beta/\eta)$. Introducing matrix notation and the rapidity $y = \ln\eta$, Eq. (2) can be simplified to read

$$\hat{F}(y, N+1) = \int_{-\infty}^{0} \hat{f}(y-y')\,\hat{F}(y', N)\,dy' , \tag{3}$$

where $\hat{F}$ are column vectors and $\hat{f}$ is a square matrix. In order to illustrate the properties of Eq. (3) we suppose that hadrons consist of quark-like clusters of type $\mathcal{P}$, $\mathcal{N}$, $\overline{\mathcal{P}}$, $\overline{\mathcal{N}}$ and a neutral gluon ϕ. Furthermore, we assume that the clusters describing the physics at each scale have these quantum numbers. Then $\hat{F}$ has the entries

$$\begin{bmatrix} \mathcal{P} \\ \mathcal{N} \\ \overline{\mathcal{P}} \\ \overline{\mathcal{N}} \\ \phi \end{bmatrix} .$$

Helicity dependence, λ quarks, etc. can be included straightforwardly. The most general form of $\hat{f}$ compatible with charge conjugation and isospin invariance is

$$\hat{f}(\beta/\eta) = \begin{bmatrix} a & b & c & d & h \\ b & a & d & c & h \\ c & d & a & b & h \\ d & c & b & a & h \\ e & e & e & e & g \end{bmatrix} , \tag{4}$$

where each entry is a positive function of longitudinal fraction. Furthermore, the entries are constrained by the conservation of longitudinal momentum—the sum of the longitudinal momenta of the type-$(N+1)$ clusters in a cluster of type N should be the longitudinal momentum of the Nth cluster,

$$\sum_i \int_0^1 f^{ij}(\eta)\,d\eta = 1 \tag{5}$$

for each j.

Equation (3) can be solved by Laplace transform as in Ref. 4. Equation (13) of that reference becomes

$$\hat{M}_\alpha(N+1) = \hat{m}_\alpha \hat{M}_\alpha(N) , \tag{6}$$

where $\hat{M}_\alpha$ and $\hat{m}_\alpha$ are the αth moments defined as

$$\hat{M}_\alpha(N) = \int_{-\infty}^{0} e^{\alpha y}\,\hat{F}(y, N)\,dy ,$$
$$\hat{m}_\alpha = \int_{-\infty}^{0} e^{\alpha y}\,\hat{f}(y)\,dy . \tag{7}$$

The solution of Eq. (6) is[4]

$$\hat{M}_\alpha(N) = (\hat{m}_\alpha)^N \hat{M}_\alpha , \tag{8}$$

where $\hat{M}_\alpha(N=0) \equiv M_\alpha$, and careted quantities indicate column vectors or square matrices.

Each matrix $\hat{m}_\alpha$ must have the form given in Eq.

(4) with positive entries everywhere. Furthermore, from Eq. (5) it follows that

$$\sum_i m^{ij}_{(\alpha=1)} = 1 \tag{9}$$

for each j. For $\alpha > 1$

$$\sum_i m^{ij}_{\alpha} < 1 \tag{10}$$

for each j.

The matrix entries of $\hat{m}_\alpha$ are monotonically decreasing functions of α. This can be seen by differentiating Eq. (7) with respect to α and recalling that $f^{ij}(y) \geq 0$. Denote the eigenvalue of $\hat{m}_\alpha$ of maximum absolute value $\lambda(\alpha)$. It follows that $\lambda(\alpha)$ is monotonically decreasing. From Eq. (9) it can be seen that

$$\lambda(1) = 1 \ . \tag{11}$$

The right and left eigenvectors, $\hat{r}(\alpha)$ and $\hat{l}(\alpha)$, associated with $\lambda(\alpha)$ have the form

$$\hat{r}(\alpha) \sim \begin{bmatrix} 1 \\ 1 \\ 1 \\ 1 \\ r(\alpha) \end{bmatrix} , \tag{12}$$

$$l(\alpha) \sim (1, 1, 1, 1, l(\alpha)) \ ,$$

where $r(\alpha), l(\alpha) > 0$. When the matrix $\hat{m}_\alpha$ is raised to a large power N, it is well approximated by

$$[m^N_\alpha]_{ij} \sim [\lambda_{(\alpha)}]^{N-1} l_j(\alpha) r_i(\alpha) \ , \tag{13}$$

where the vectors $\hat{r}(\alpha)$ and $\hat{l}(\alpha)$ are normalized by

$$r_i(\alpha) l_i(\alpha) = \lambda(\alpha) \ . \tag{14}$$

Equation (8) can now be analyzed in more detail. From Eq. (13) it follows that

$$\hat{M}_\alpha(N) \sim [\lambda(\alpha)]^{N-1} l_i(\alpha) M_{\alpha i} \hat{r}(\alpha) \ . \tag{15}$$

Using the connection between N and Q^2, the Q^2 dependence of Eq. (15) can be made explicit:

$$\hat{M}_\alpha(Q^2) \sim (Q^2/\xi^2)^{-d_\alpha} [\lambda^{-1}(\alpha) l_i(\alpha) M_{\alpha i}] \hat{r}(\alpha) \ , \tag{16}$$

where

$$d_\alpha = -\ln\lambda(\alpha)/\ln\Lambda^2 \ . \tag{17}$$

Note that for large N the ratios of moments of the distributions of partons of different types i become independent of the hadron, and that the moments of the $\mathcal{P}$, $\mathfrak{N}$, $\bar{\mathcal{P}}$, and $\bar{\mathfrak{N}}$ distribution functions become equal. For the case $\alpha = 1$, $\lambda(1) = 1$, so that Eq. (16) becomes independent of Q^2:

$$M_{(\alpha=1)}(Q^2) = \text{const}$$

or

$$\int_0^1 F_i(\eta, Q^2)\, d\eta = \text{const} \ , \tag{18}$$

for $i = \mathcal{P}, \mathfrak{N}, \bar{\mathcal{P}}, \bar{\mathfrak{N}}$. This means physically that $\mathcal{P}$, $\mathfrak{N}$, $\bar{\mathcal{P}}$, and $\bar{\mathfrak{N}}$ clusters of type N (for N sufficiently large) each carry equal longitudinal fractions of the hadron's infinite momentum. The gluon clusters of type N must carry the remaining longitudinal fraction available. We finally note that the moments of the difference of distribution functions, such as $\mathcal{P} - \bar{\mathcal{P}}$, are controlled by lower eigenvalues of $\hat{m}_\alpha$ and necessarily fall faster than the $\mathcal{P}$ and $\bar{\mathcal{P}}$ moments themselves.

Other quantum-number constraints on $\hat{f}$ and $\hat{F}$ follow from isospin and baryon-number considerations. The total isospin of the clusters of type $N+1$ in a cluster of type N should sum to the isospin of the cluster of type N. For example, choosing the cluster of type N to have the quantum numbers of a $\mathcal{P}$ quark,

$$\int [f^{\mathcal{P}\mathcal{P}}(y) - f^{\mathfrak{N}\mathcal{P}}(y) + f^{\bar{\mathfrak{N}}\mathcal{P}}(y) - f^{\bar{\mathcal{P}}\mathcal{P}}(y)]\, dy = 1 \ ,$$

$$\int [f^{\mathcal{P}\mathcal{P}}(y) + f^{\mathfrak{N}\mathcal{P}}(y) - f^{\bar{\mathfrak{N}}\mathcal{P}}(y) - f^{\bar{\mathcal{P}}\mathcal{P}}(y)]\, dy = 1 \ .$$

The initial structure functions $F_i(y, N=1)$ must be normalized to the total isospin and baryon number of the proton, say,

$$\int [F_{\mathcal{P}}(y, N=1) - F_{\mathfrak{N}}(y, N=1) - F_{\bar{\mathcal{P}}}(y, N=1) + F_{\bar{\mathfrak{N}}}(y, N=1)]\, dy = 1 \ , \tag{19}$$

$$\int [F_{\mathcal{P}}(y, N=1) + F_{\mathfrak{N}}(y, N=1) - F_{\bar{\mathcal{P}}}(y, N=1) - F_{\bar{\mathfrak{N}}}(y, N=1)]\, dy = 1 \ .$$

Using the iteration formula (3), it is easy to see that $N=1$ can be replaced by arbitrary N in Eq. (19). When the distribution functions $\hat{F}$ are used in the scale-invariant parton model to calculate neutrino structure functions, as in Sec. IV, Eq. (19) becomes equivalent to the Adler sum rule. Thus, the theory developed here guarantees the validity of current-algebra sum rules.

III. MOMENTUM-SLICED MODELS AND THE IMPULSE APPROXIMATION

We would like to apply the distribution functions $F_i(y, N)$ to deep-inelastic lepton scattering problems. To do this we must show that the impluse approximation remains uniformly valid as the external probe resolves smaller and smaller scales. Throughout Ref. 4 and the preceding discussion we

have imagined that the ratio between different length scales is large. Then wavelengths of an external probe can be chosen such that the probe resolves the distance between clusters of type N but sees individual clusters of type N as pointlike. In order to use the impulse approximation in describing the interactions of the probe with clusters of type N, it is necessary that the time over which the probe acts be small in comparison with times characterizing the interactions between the clusters being probed. In the conventional parton model[7] the time over which the probe acts is of order ν^{-1}. The time scale for interactions between partons of longitudinal fraction η behaves as η/κ^2, where κ is the transverse momentum fluctuations of the partons. Therefore, the impulse approximation is valid when

$$\frac{1}{\nu} \ll \frac{\eta}{\kappa^2} ;$$

that is,

$$Q^2 \gg \kappa^2 . \tag{20}$$

Therefore, the impulse approximation remains good whenever Q^2 is large enough regardless of the longitudinal fraction η of the parton being probed.

In the scale-invariant parton model the transverse-momentum fluctuations of clusters of type N grow as the reciprocal of the distance between them. Thus, the condition that $Q^2 \gg \kappa^2$ is *identical* to the requirement that the external probe be able to resolve the spatial distribution of the partons.

It is instructive to divide the Q^2-ν plane into bands denoting the individual scaling regions (Fig. 1). In the interior of these bands, i.e., $\Lambda^N \ll Q \ll \Lambda^{N+1}$, one can apply the naive parton model. Along

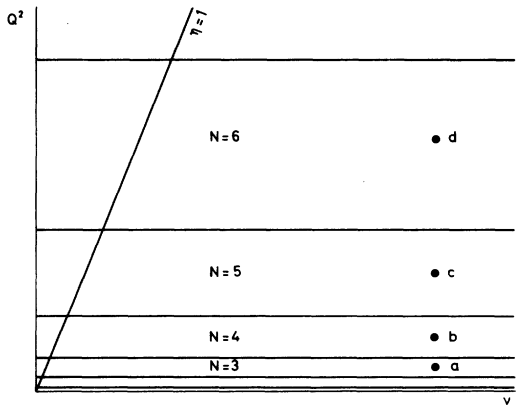

FIG. 1. The Q^2-ν plane divided into bands. The impulse approximation has equal validity for all ν at fixed Q^2. It also has equal validity at corresponding points such as a, b, c, and d in different bands.

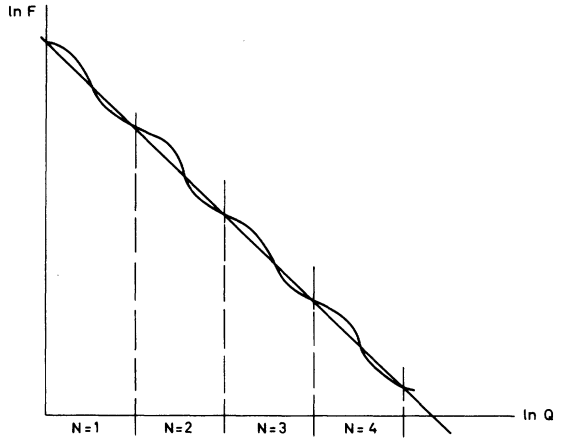

FIG. 2. Variation of various quantities will average to power laws in Q^2 when averaged over several scales.

the length of each band the impulse approximation remains uniformly good. This follows from the η independence of Eq. (20). Since each band is a rescaled replica of any other, the impulse approximation is equally valid at corresponding points in different bands. This does not mean that the impulse approximation is perfect in each band. Instead, the average percentage error in each band is independent of the particular band chosen. Therefore, the errors incurred from our use of the impulse approximation should be independent of Q^2 and η.

Since the impulse approximation should give the correct behavior for scattering amplitudes up to errors of normalization, the power laws of the distribution function $F_i(y, Q^2)$ must be identical (apart from kinematic factors) to the power laws of the measurable scattering amplitudes. At the same time, however, the constants of proportionality between the measurable quantities and the distribution functions cannot be determined easily. This situation is analogous to that in statistical-mechanics studies of systems near a critical point. Here power laws of thermodynamic functions such as spin-spin correlation functions can be determined very accurately, but the strength of those functions cannot usually be obtained so simply.

When Q^2 varies between scaling regions, the scale-invariant parton model typically predicts power behavior for functions of interest (such as the moments of the structure functions). These power laws average the actual Q^2 dependence over many scales as depicted in Fig. 2. In scale-invariant field theories we do not necessarily expect discrete transitions between different scaling regions. We do feel, however, that the average features (indices of power laws, for example) can be obtained correctly by the "momentum-slice"

techniques referred to here.[8]

Renormalizable field theories which are not scale-invariant are probably more difficult to analyze. In this case the dimensionless coupling constants describing the interactions between clusters will vary from level to level and perhaps become infinite. The time scales governing the interactions between clusters of type N will then decrease at a faster rate than the distances between clusters of type N. This leads to an increasing violation of Eq. (20) as Q^2 increases.

IV. DEEP-INELASTIC SCATTERING

We will now discuss a class of applications to deep-inelastic lepton-hadron reactions. In particular, we are interested in quantities, such as cross sections and energy losses, which are very accessible experimentally. Define averages of quantities such as

$$\sigma(E)\langle(Q^2)^a\eta^c\rangle \equiv \int (Q^2)^a \eta^c \frac{d\sigma}{dQ^2 d\nu} dQ^2 d\nu \qquad (21)$$

as a function of the incident neutrino energy E. For example, setting $a=c=0$ defines the total neutrino cross section. The case $a=1$, $c=0$ is related to the mean invariant momentum squared transferred to the leptons, and the case $a=1$, $c=-1$ is related to the mean energy loss suffered by the leptons, etc. As discussed above, we assume that naive parton ideas can be used when the wavelength of the incident current is larger than the probed clusters but much smaller than the distances between them, i.e., $\Lambda^N \ll Q \ll \Lambda^{N+1}$. The naive parton expressions for neutrino and antineutrino differential cross sections read[9]

$$\nu\frac{d\sigma^\nu}{dQ^2 d\nu} = \frac{G^2\cos^2\theta_c}{\pi}\left[F_{\mathfrak{N}}(\eta) + \left(1-\frac{Q^2}{2E}\right)^2 F_{\bar{\mathfrak{P}}}(\eta)\right],$$
$$\nu\frac{d\sigma^{\bar\nu}}{dQ^2 d\nu} = \frac{G^2\cos^2\theta_c}{\pi}\left[F_{\bar{\mathfrak{P}}}(\eta) + \left(1-\frac{Q^2}{2E}\right)^2 F_{\mathfrak{N}}(\eta)\right]. \qquad (22)$$

In the naive parton model the $Q^2/2E$ terms in Eq. (22) contribute significantly to the total cross sections. However, as shown in the Appendix, the average $\langle Q^2/2E\rangle$ falls as a power of E in the scale-invariant parton model. Therefore, partons and antipartons contribute with equal weights to the neutrino and antineutrino total cross sections, and Eq. (22) becomes

$$\frac{d\sigma^\nu}{dQ^2 d\eta} \approx \frac{G^2\cos^2\theta_c}{\pi}\left[\frac{F_{\mathfrak{N}}(\eta, N)}{\eta} + \frac{F_{\bar{\mathfrak{P}}}(\eta, N)}{\eta}\right],$$
$$\frac{d\sigma^{\bar\nu}}{dQ^2 d\eta} \approx \frac{G^2\cos^2\theta_c}{\pi}\left[\frac{F_{\bar{\mathfrak{P}}}(\eta, N)}{\eta} + \frac{F_{\mathfrak{N}}(\eta, N)}{\eta}\right], \qquad (23)$$

where $F_i(\eta, N)$ is the distribution function for clusters of type i and size $R_N \sim \Lambda^{-N} \sim Q^{-1}$. In the Appendix we evaluate Eq. (21) by approximating the Q^2 integral by a summation over the distinct scaling regions $N=1, 2, \ldots, \ln(2\eta E)/\ln\Lambda^2$ followed by the appropriate integral over η. This calculation is carried out using the iteration formula (3) which allows us to relate adjoining scaling regions N and $N+1$. The following results emerge:

$$\sigma(E)\langle(Q^2)^a\eta^c\rangle \sim E^b , \qquad (24)$$

where the power index b satisfies

$$b = G(a+c+1) - c . \qquad (25)$$

Equation (25) and the properties of G are discussed in detail in the Appendix. In particular, $G(a+1)-a$ is a decreasing function of its argument, so the higher moments of $\langle(Q^2)^a/E^a\rangle$ fall more and more rapidly with E. Of special interest are the total neutrino and antineutrino cross sections. We find that $G(1)=1$, so

$$\sigma_{\rm tot}^{\nu,\bar\nu}(E) \sim \text{const}\times E + \text{lower-order terms} . \qquad (26)$$

This simple result can be understood intuitively as the compensation between two effects. As N increases the mean longitudinal fraction of a cluster decreases, lowering its contribution to the cross section. However, as N increases the number of clusters resolved increases, and the two effects precisely cancel. In the naive parton model $\sigma_{\rm tot}^{\nu,\bar\nu}(E)$ are also proportional to E, as can be guessed by dimensional analysis.[9] Therefore, the presence of a linear rise of $\sigma^{\nu,\bar\nu}$ with E should not necessarily be interpreted as evidence for canonical scaling. However, if the antipartons in protons and neutrons carry negligible longitudinal momentum, then the naive parton model predicts $\sigma^{\bar\nu T}/\sigma^{\nu T} \approx \frac{1}{3}$ if the target T consists of equal numbers of protons and neutrons.[9] In the scale-invariant model one also expects a large asymmetry of this type when N is small. However, as N grows (i.e., enormous values of Q^2) and smaller clusters are resolved, scale invariance implies that the moments of the distribution functions of clusters of different types i become equal [Eq. (16)]. Since σ^ν and $\sigma^{\bar\nu}$ receive their dominant contributions from Q^2 values which increase with E, it is clear why $\sigma^{\bar\nu}/\sigma^\nu$ tends to unity as $\ln Q^2$ becomes very large (Fig. 3).

It is also interesting to consider the total electroproduction cross section, which can be obtained from the $a=-2$, $c=0$ case of Eq. (24).[10] According to the discussion in the Appendix there are two possible behaviors for $\sigma_{\rm tot}^{ep}(E)$. If the iteration function $\hat f$ is nonvanishing at $\eta=0$, then $G(-1)$ is positive. This implies that $\sigma_{\rm tot}^{ep}(E)$ grows as E^b,

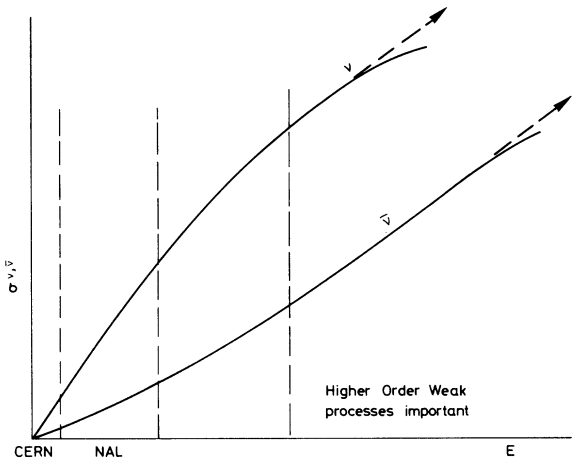

FIG. 3. Energy dependence of neutrino and antineutrino cross sections averaged over proton and neutron targets. The dashed lines extrapolate the lowest-order weak process.

$0<b<1$. However, if $\hat{f}(0)=0$, then $G(-1)$ may be either positive or zero depending on the details of the moments of $\hat{f}$. If $G(-1)$ is zero, the total cross section may tend to a constant or some power of $\ln E$ as in the naive parton model.[7]

Two kinematic quantities which are easily measured in neutrino deep-inelastic reactions are the average energy loss of the leptons $\langle \nu(E)\rangle$ and the average invariant momentum transfer squared $\langle Q^2(E)\rangle$. Choosing $a=1$ and $c=-1$ in Eq. (24) and referring to the Appendix, we have

$$\langle \nu(E)\rangle \sim E. \tag{27}$$

This agrees with the analysis of the naive parton model and hence is not a sensitive probe into the validity of Bjorken scaling. A more sensitive quantity is $\langle Q^2/2E\rangle$ which is constant in the naive parton model. Choosing $a=1$ and $c=0$ in Eq. (24), however, gives

$$\langle Q^2/2E\rangle \sim E^{p-1}, \quad 0<p<1\ . \tag{28}$$

For presently accessible values of Q^2 and E, it is known that $\langle Q^2/2E\rangle \approx \frac{1}{9}$ for neutrino processes.[11] If and when canonical scaling begins to break down in the way envisioned in the scale-invariant parton model, this quantity should begin to decrease. The fact that $\langle Q^2/2E\rangle$ falls as a power of E also justifies our neglect of the $Q^2/2E$-dependent terms in Eq. (22).

An interesting question in the scale-invariant parton model is whether symmetry breaking disappears at short distances.[12] This is the case in many models of SU(3)-symmetry breaking. For such theories the iteration matrix (suitably generalized to include λ quarks) will be symmetric with respect to $\mathcal{P}$, $\mathfrak{N}$, and λ quarks. Thus, the eigenvector corresponding to the maximum eigenvalue of the moment matrices of $\hat{f}$ will have equal entries for $\mathcal{P}$, $\mathfrak{N}$, and λ. This means that after many iterations, the ratio of the distribution functions of $\mathcal{P}$, $\mathfrak{N}$, and λ quarks must tend to unity for all hadrons. Moreover, the matrix elements of the currents (Cabibbo angle) will not change from scale to scale. This is, of course, due to the fact that matrix elements of conserved currents are not renormalized.

The strangeness-changing neutrino-nucleon cross section is given by Eq. (23) with the replacements $G\cos\theta_C \to G\sin\theta_C$ and $\mathfrak{N}$ quark $\to \lambda$ quark. Since the ratio of the distribution functions of $\mathfrak{N}$ and λ quarks tend to unity after many iterations, the only difference between strangeness-conserving and strangeness-changing cross sections comes from the Cabibbo angle. Thus, when $\ln E$ becomes large,

$$\frac{\sigma^{\nu}(\Delta S=1)}{\sigma^{\nu}(\Delta S=0)} \to \tan^2\theta_C\ . \tag{29}$$

If, on the other hand, SU(3)-breaking effects do not disappear at short distances, the ratio $\sigma^{\nu}(\Delta S=1)/\sigma^{\nu}(\Delta S=0)$ may vary as a power of E. This would be due to a change of coupling strength of the strangeness-changing current as smaller and smaller distances are probed. This phenomenon was discussed in Ref. 4.

Finally, it is important to emphasize that the violations of canonical scaling contained in the scale-invariant parton model are characteristically different from those which would occur if the weak and/or electromagnetic interactions were mediated by a heavy fundamental intermediate vector meson. The effect of such vector mesons of mass M_W will be to multiply the canonical structure functions $F_2(\eta)$ by decreasing functions of Q^2.[13] Thus, for example, the area under the structure functions as well as all other moments would fall to zero uniformly with Q^2. In addition, the total neutrino-nucleon cross section would deviate from the linear function of E, becoming a linear function of $\ln E$ for $E \gg M_W$.[9] These results are clearly in sharp contrast with those obtained in the model discussed here.

V. CONCLUSIONS

We conclude with a summary of our experimentally interesting results.

(1) The total neutrino and antineutrino cross sections should rise linearly with E. As E grows, the ratio of neutrino to antineutrino cross sections should approach unity. This is part of the more general phenomenon that ratios of the moments of the distribution functions of $\mathcal{P}$, $\mathfrak{N}$, $\bar{\mathcal{P}}$, and $\bar{\mathfrak{N}}$ clus-

ters approach unity as Q^2 increases.

(2) The mean energy loss $\langle \nu(E) \rangle$ of the leptons in neutrino and antineutrino scattering grows linearly with E. The mean invariant momentum transfer squared $\langle Q^2(E) \rangle$ of the leptons grows as E^p, $0<p<1$. This second prediction provides a relatively easy test for the breakdown of canonical scaling which predicts $\langle Q^2(E) \rangle \sim E$.

(3) A test of SU(3) symmetry at short distances can be made if it becomes possible to identify the strangeness-changing cross section $\sigma^\nu(\Delta S=1)$ and the strangeness-conserving cross section $\sigma^\nu(\Delta S=0)$. If SU(3) is valid at short distances, then $\sigma^\nu(\Delta S=1)/\sigma^\nu(\Delta S=0) \to \tan^2\theta_C$.

(4) We finally stress that these results apply when Q^2 and ν become so large that their logarithms can also be considered large, but not so large that modifications of the current-current form of weak interactions become important. This may in fact be a narrow energy region, but perhaps it is large enough so that deviations from canonical scaling can be observed.

ACKNOWLEDGMENT

One of us (J. K.) would like to thank his colleagues at Tel Aviv University for their hospitality.

APPENDIX

It is the purpose of this appendix to determine the energy dependence of the quantities

$$\sigma(E)\langle (Q^2)^a \eta^c \rangle \equiv \int \frac{d\sigma}{dQ^2 d\nu} (Q^2)^a \eta^c \, dQ^2 d\nu \,, \qquad \text{(A1)}$$

where $d\sigma/dQ^2 d\nu$ is the neutrino-hadron differential cross section. The naive-parton-model expression for the spin-averaged differential cross section reads

$$\eta \frac{d\sigma}{dQ^2 d\eta} = \frac{G^2 \cos^2\theta_C}{\pi} \left[F_{\mathfrak{N}}(\eta) + \left(1 - \frac{Q^2}{2E}\right)^2 F_{\bar{\mathfrak{N}}}(\eta) \right] . \qquad \text{(A2)}$$

In the scale-invariant parton model the distribution functions F_i should refer to clusters of type $N = \ln(Q^2/\xi^2)/\ln\Lambda^2$. We shall see that the $Q^2/2E$ terms in this formula become negligible compared to the other terms when $E \to \infty$. Therefore, Eq. (A2) can be simplified to

$$\eta \frac{d\sigma}{dQ^2 d\eta} \approx \frac{G^2 \cos^2\theta_C}{\pi} \left[F_{\mathfrak{N}}(\eta, N) + F_{\bar{\mathfrak{N}}}(\eta, N) \right] . \qquad \text{(A3)}$$

Similarly, for antineutrino scattering,

$$\eta \frac{d\bar{\sigma}}{dQ^2 d\eta} \approx \frac{G^2 \cos^2\theta_C}{\pi} \left[F_{\bar{\mathfrak{N}}}(\eta, N) + F_{\mathfrak{N}}(\eta, N) \right] . \qquad \text{(A4)}$$

In addition there are corrections to these formulas due to the fact that the mean transverse momentum fluctuations of clusters grow with N. These effects influence the helicity structure of Eqs. (A3) and (A4), but do not change the power laws which will be obtained below.[14] Substituting Eq. (A3) into Eq. (A1) gives

$$\sigma(E)\langle (Q^2)^a \eta^c \rangle \cong \frac{G^2 \cos^2\theta_C}{\pi} \int (Q^2)^a \eta^c \left[F_{\mathfrak{N}}(\eta, N) + F_{\bar{\mathfrak{N}}}(\eta, N) \right] dQ^2 \frac{d\eta}{\eta} . \qquad \text{(A5)}$$

Define

$$\sigma(E)\langle (Q^2)^a \eta^c \rangle_i = \frac{G^2 \cos^2\theta_C}{\pi} \int (Q^2)^a \eta^c F_i(\eta, N) \, dQ^2 \frac{d\eta}{\eta} . \qquad \text{(A6)}$$

According to the scale-invariant parton model, the functions $F_i(\eta, N)$ depend only on η when Q^2 lies between scales Λ^{2N} and $\Lambda^{2(N+1)}$. Therefore, Eq. (A6) becomes

$$\sigma(E)\langle (Q^2)^a \eta^c \rangle_i \approx \frac{G^2 \cos^2\theta_C}{\pi} \int \sum_{N=1}^{N_{\max}} \Lambda^{2(a+1)N} (1 - \Lambda^{-2(a+1)}) \times F_i(\eta, N) \eta^c \frac{d\eta}{\eta} , \qquad \text{(A7)}$$

where $N_{\max} = \ln(2\eta E)/\ln\Lambda^2$. Define $\kappa = \ln E/\ln\Lambda^2$. We shall determine the behavior of Eq. (A7) as a function of E, the incident neutrino energy. In terms of the rapidity variable $y = \ln\eta$, Eq. (A7) becomes

$$\sigma(E)\langle (Q^2)^a \eta^c \rangle_i \approx \frac{G^2 \cos^2\theta_C}{\pi} \int e^{cy} \sum_{N=1}^{\kappa + y/\ln\Lambda^2} \Lambda^{2(a+1)N} (1 - \Lambda^{-2(a+1)}) \times F_i(\eta, N) \, dy . \qquad \text{(A8)}$$

Define an additional function

$$\mathfrak{F}_i(y, \kappa + y/\ln\Lambda^2) = \sum_{N=1}^{\kappa + y/\ln\Lambda^2} \Lambda^{2(a+1)N} (1 - \Lambda^{-2(a+1)}) \times F_i(y, N) . \qquad \text{(A9)}$$

Recall the recursion formula (3),

$$\hat{F}(y, N+1) = \int_{-\infty}^{0} \hat{f}(y - y') \hat{F}(y', N) \, dy' . \qquad \text{(A10)}$$

Multiplying by $\Lambda^{2(a+1)(N+1)} (1 - \Lambda^{-1})$ and summing over N, we can obtain a recursion relation for $\int e^{cy} \hat{\mathfrak{F}} \, dy$,

$$\int e^{cy}\,\hat{\mathfrak{F}}(y,\kappa+y/\ln\Lambda^2+1)\,dy=\Lambda^{2(a+1)}\int \hat{f}(y-y')\,e^{cy}\,\hat{\mathfrak{F}}(y',\kappa+y/\ln\Lambda^2)\,dydy'-\Lambda^{2(a+1)}(1-\Lambda^{-2(a+1)})\hat{K}\ , \tag{A11}$$

where $\hat{K}$ is a constant matrix. Differentiating Eq. (A11) with respect to κ,

$$\frac{\partial}{\partial\kappa}\int e^{cy}\,\hat{\mathfrak{F}}(y,\kappa+y/\ln\Lambda^2+1)\,dy=\Lambda^{2(a+1)}\int \hat{f}(y-y')\,e^{cy}\frac{\partial}{\partial\kappa}\,\hat{\mathfrak{F}}(y',\kappa+y/\ln\Lambda^2)\,dydy'\ . \tag{A12}$$

Shifting the κ differentiation to the variable y on the right-hand side and integrating by parts, we obtain

$$\frac{\partial}{\partial\kappa}\int e^{cy}\,\hat{\mathfrak{F}}(y,\kappa+y/\ln\Lambda^2+1)\,dy=\Lambda^{2(a+1)}\ln\Lambda^2\int\frac{\partial}{\partial y'}\hat{f}(y-y')\,e^{cy}\,\hat{\mathfrak{F}}(y',\kappa+y/\ln\Lambda^2)\,dydy'$$

$$-c\,\Lambda^{2(a+1)}\ln\Lambda^2\int\hat{f}(y-y')\,e^{cy}\,\hat{\mathfrak{F}}(y',\kappa+y/\ln\Lambda^2)\,dydy'\ . \tag{A13}$$

Represent the function $\hat{f}$ by a sum of step functions,

$$\hat{f}(y)=\int\hat{c}(u)\,e^{u}\,\theta(y+u)\,du\ , \tag{A14}$$

where

$$\hat{c}(y)=\frac{\partial}{\partial\eta}\hat{f}(\eta)$$

and the moments of $\hat{f}$ can be expressed as

$$\alpha\hat{m}_\alpha=\int e^{u(1-\alpha)}\,\hat{c}(u)\,du\ . \tag{A15}$$

Equation (A13) becomes

$$\frac{\partial}{\partial\kappa}\int e^{cy}\,\hat{\mathfrak{F}}(y,\kappa+y/\ln\Lambda^2+1)\,dy=\Lambda^{2(a+1)}\ln\Lambda^2\int\hat{c}(u)\,e^{u}\,\delta(y-y'+u)\,e^{cy}\,\hat{\mathfrak{F}}(y',\kappa+y/\ln\Lambda^2)\,dydy'du$$

$$-c\ln\Lambda^2\int e^{cy}[\hat{\mathfrak{F}}(y,\kappa+y/\ln\Lambda^2+1)+\Lambda^{2(a+1)}(1-\Lambda^{-2(a+1)})\hat{K}]\,dy\ , \tag{A16}$$

which can be written

$$\frac{\partial}{\partial\kappa}[\sigma(E)\langle(Q^2)^a\eta^c\rangle_i]\Big|_{\kappa+1}=\Lambda^{2(a+1)}\ln\Lambda^2\int e^{(1-c)u}\,c_{ij}(u)[\sigma(E)\langle(Q^2)^a\eta^c\rangle_j]\,|_{\kappa-u/\ln\Lambda^2}\,du$$

$$-c\ln\Lambda^2[\sigma(E)\langle(Q^2)^a\eta^c\rangle_i]\,|_{\kappa+1}-\frac{G^2\cos^2\theta_c}{\pi}(\Lambda^{2(a+1)}-1)(\ln\Lambda^2)K_i\ . \tag{A17}$$

In all but one of the cases to be studied each term in this equation will grow with E except the last. Ignoring the last term, solutions to Eq. (A17) have the form

$$\sigma(E)\langle(Q^2)^a\eta^c\rangle_i\,|_\kappa=e^{b(\ln\Lambda^2)\kappa}v_i\ . \tag{A18}$$

Substituting into Eq. (A17) gives

$$(b+c)\,v_i=\Lambda^{2(a-b+1)}\int e^{(1-c-b)u}\,c_{ij}(u)\,v_j\,du\ . \tag{A19}$$

Equation (A15) allows Eq. (A19) to be written in terms of $\hat{f}$:

$$v_i=\Lambda^{2(a-b+1)}\hat{m}_\alpha^{ij}\,v_j\ . \tag{A20}$$

The leading-power behaviors of the quantities of interest are controlled by the largest eigenvalues of $\hat{m}_\alpha$. Therefore, Eq. (A20) becomes

$$\Lambda^{-2(a-b+1)}=\lambda(b+c)\ . \tag{A21}$$

It is convenient to define numbers

$$B=b+c,\quad A=a+c+1 \tag{A22}$$

so that the logarithm of Eq. (A21) becomes

$$2(B-A)\ln\Lambda=\ln\lambda(B)\ . \tag{A23}$$

Note that $\ln\lambda(B)$ is a monotonically decreasing function of B which passes through zero at $B=1$. If $\hat{f}(\eta)$ vanishes at $\eta=0$, then $\lambda(0)$ is finite. If $\hat{f}(0)\neq0$ then $\lambda(0)$ is divergent. These two cases are plotted along with graphs of $2(B-A)\ln\Lambda$ in Figs. 4(a) and 4(b). From this we read off the solutions

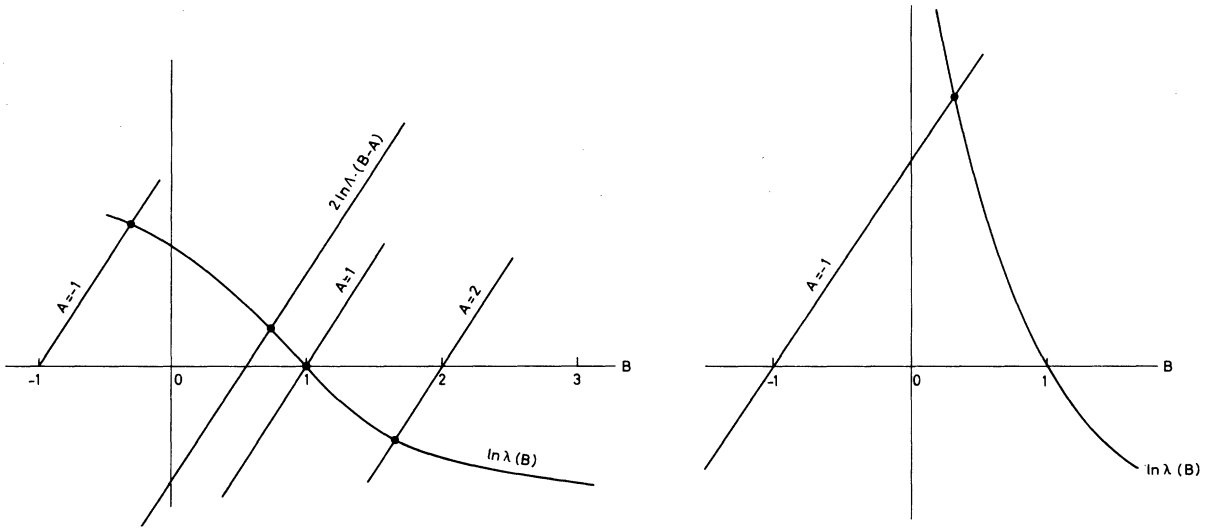

FIG. 4. (a) The functions $\ln\lambda(B)$ and $2(B-A)\ln\Lambda$ for the case $\hat{f}(\eta=0)=0$. (b) Same as (a) except $\hat{f}(\eta=0)\neq 0$.

$$\sigma(E)\sim E \qquad (a=0,\ c=0),$$

$$\langle\nu\rangle\sim E \qquad (a+1,\ c=-1), \qquad \text{(A24)}$$

$$\langle Q^2\rangle\sim E^p,\quad 0<p<1 \qquad (a=1,\ c=0)\ .$$

When A is less than zero, the analysis of Eq. (A23) is more complicated. The curve $2(B-A)\ln\Lambda$ may intersect the curve $\ln\lambda(B)$ at positive or negative values of B. If $\hat{f}(0)\neq 0$, then the intersection must occur for positive values of B. If $\hat{f}(\eta)$ vanishes at $\eta=0$, then negative values of B are apparently possible. However, in this case the constant term in Eq. (A17) becomes important and leads to constant energy dependence. These results are discussed in detail in the text.

*Work supported in part by the Israel Academy of Sciences.

[1]Studies of the breakdown of canonical scaling in perturbation theory have been made by many authors. Some recent works include M. Kugler and S. Nussinov, Nucl. Phys. B28, 97 (1971); V. Gribov and L. Lipatov, Phys. Lett. 37B, 63 (1971); N. Christ, B. Hasslacher, and A. Mueller, Phys. Rev. D 6, 3543 (1972). More general field-theoretic studies have been made by K. G. Wilson [Phys. Rev. 179, 1499 (1969)]. Considerable pioneering work has also been done by A. M. Polyakov and A. A. Migdal; see, for example, Zh. Eksp. Teor. Fiz. 60, 1572 (1971) [Sov. Phys.—JETP 33, 850 (1971)] and references cited therein.

[2]Field theories with underlying gauge symmetries (for example, quantum electrodynamics) may have more subtle short-distance behavior than that envisioned here.

[3]For a summary of model results see K. G. Wilson, invited talk presented at the XVI International Conference on High Energy Physics, Chicago-NAL, Batavia, Ill., 1972 (unpublished). Some of these results are illustrated in K. G. Wilson and J. Kogut, IAS Report No. COO-2220-2 (unpublished).

[4]J. Kogut and Leonard Susskind, Phys. Rev. D 9, 697 (1974).

[5]C. H. Llewellyn Smith, Phys. Rep. 3C, No. 5 (1972).

[6]Our kinematic conventions are the following. In a deep-inelastic process ν + hadron$\rightarrow\mu$ + anything, q denotes the momentum transferred from the leptons to the hadrons. E is the energy of the neutrino in the lab, and ν is the energy loss suffered by the leptons in the collision. In the deep-inelastic limit Q^2 and ν approach infinity while their ratio is held fixed. Infinite-momentum frames are defined in Ref. 7.

[7]J. Kogut and Leonard Susskind, Phys. Rep. 8C, 75 (1973).

[8]Momentum-space slicing techniques useful for analyzing renormalizable field theories were introduced by K. Wilson [Phys. Rev. 140, 445 (1965)].

[9]J. D. Bjorken and E. A. Paschos, Phys. Rev. D 1, 3151 (1970). For a recent review of neutrino physics and parton models see E. A. Paschos, invited talk presented at the New York meeting of the American Physical Society, 1973 (unpublished); NAL report, 1973 (unpublished).

[10]In this case different combinations of structure functions enter the expression for the differential cross section. These modifications do not change the conclusions reached in the text.

[11]G. Wyatt and D. H. Perkins, Phys. Lett. 34B, 542 (1971).

[12]For example, see the discussion of skeleton theories by K. Wilson [Phys. Rev. 179, 1499 (1969)].

[13]One such model has been discussed recently by M. S. Chanowitz and S. D. Drell [Phys. Rev. Lett. 30, 807 (1973)].

[14]For example, because of large transverse-momentum fluctuations $\mathcal{P}$- and $\mathfrak{N}$-type clusters can contribute to neutrino scattering. See the discussion of $R=\sigma_S/\sigma_T$ in Ref. 4.